Clays and Clay Minerals, Vol. 56, No. 5, 505–510, 2008.

CHANGE OF THE REFRACTIVE INDEX OF ILLITE PARTICLES BY REDUCTION OF THE Fe CONTENT OF THE OCTAHEDRAL SHEET

FRANK FRIEDRICH*, ANNETT STEUDEL, AND PETER G. WEIDLER

Division of Nanomineralogy, Institute for Technical Chemistry – Water and Geotechnology (ITC-WGT), Forschungszentrum Karlsruhe GmbH, Germany

Abstract—Sub-micrometer clay particles are of interest in clay-polymer applications, especially when transparency is important. The scattering of light can be reduced by the adjustment of the refractive index (RI) of the clays to that of the matrix. In this study, the RI of sub-micrometer illite particles was changed by treatment with 5 M HCl for treatment times ranging between 2 and 24 h. The dissolution of Fe leads to a decrease in the RI of illite from 1.587 for the unaltered material to 1.502 after 24 h. The layer structure of the illite particles was preserved during the treatment. The RI of the sub-micrometer illite particles was determined by means of a photospectrometer measuring the light intensity passing through suspensions containing the clay particles, with varying refractive indices.

Key Words—Clay, Layer Silicates, Nanocomposites, Optical Properties, Refractive Index, Small Particles.

INTRODUCTION

Clay particles are used increasingly as fillers in polymers (Alexandre and Dubois, 2000; Zeng *et al.*, 2005; Aranda *et al.*, 2006; Okada and Usuki, 2006); the optical properties of the composites are important in applications (*e.g.* Tetsuka *et al*., 2007) such as food packaging, where the clay filler should not change color or transparency, but should increase UV protection and thermal stability (Avella *et al*., 2005; Rhim and Ng, 2007).

To achieve transparency, two pathways are possible: one is the reduction in particle size to well below the wavelength of light, *i.e.* <100 nm; the other is to match the RI of the particles with that of the matrix.

Determination of the RI for sub-micrometer-sized particles is difficult using standard microscopic techniques, such as the Becke line method (Bloss, 1999) or central focal masking (Wilcox, 1983). Weidler and Friedrich (2007) described a method for determining the RI of particles of less than a few micrometers in size. A similar approach was published by Nussbaumer *et al.* (2005) for rough, transparent solids.

The particles of interest are mixed into a suspension of known RI. These RI mixtures can be prepared by mixing different amounts of two immersion oils, the RI values of which are well known. By measuring the intensity of the transmitted light in relation to the RI of the mixtures, and fitting a Gaussian curve to these data, a mean RI of the particles is readily calculated. The RI obtained is a mean of the three major refraction values, commonly found for clays, reflecting the direction dispersion of the major optical axis within the suspension.

Since the RI is, at a first approximation, a function of the electron density of the material at constant wavelengths (Feynman *et al.*, 1991), removal of atoms with a high electron density, such as Fe in clays, should have a major impact on the RI of the clay. Controlled acid attack on the metal cations in octahedral positions is a good way of reducing the electron density locally and to maintain the layer structure of the clay. The latter is an important requirement for the application as a functionalized filler in nanocomposites.

This study presents RI data of sub-micrometer-sized illite undergoing a controlled dissolution of Fe in octahedral sites by HCl.

MATERIAL AND METHODS

The illite used in this study was a commercial product of B+M, Arginotec NX, which contains illite, phlogopite, kaolinite, calcite, and traces of feldspars, quartz, apatite, and anhydrite (Table 1). Details of its origin can be found in Gilg *et al.* (1997).

Two grams of illite were dispersed in 50 mL of 5 M HCl, stored at 60ºC without agitation for 2, 4, 8, 12, and 24 h, and then washed thoroughly and freeze dried. 5 M HCl was chosen because illite is known to be more resistant to weathering than other layer silicates (Scott and Smith, 1966; Köhler *et al.*, 2003).

The Fe content was determined by X-ray fluorescence using a MagiXPRO spectrometer from Philips. For the measurements, melt tablets were formed by mixing 0.8 g of sample powder with 4.8 g of $Li_2B_4O_7$ (Spektromelt A10 from Merck).

* E-mail address of corresponding author:
frank.friedrich@itc-wgt.fzk.de
DOI: 10.1346/CCMN.2008.0560503

Table 1. Mineral composition of the starting material before and after acid treatment, determined by quantitative XRD analysis (wt.%; data normalized to kaolinite).

Mineral	Start	2 h	4 h	8 h	12 h	24 h
Illite	76.4	39.4	36.9	32.7	30.3	26.1
Phlogopite	7.8	3.2	0	0	0	0
Kaolinite	5.4	5.4	5.4	5.4	5.4	5.4
K-feldspar (orthoclase)	4.4	3.6	2.8	2.6	2.5	2.5
Calcite	2.4	0	0	0	0	0
Anhydrite	1.4	0.9	0.8	0.8	0.5	0.6
Plagioclase (Ca-rich)	1.1	1.2	1.2	1.2	1.1	0.6
Apatite	0.7	0	0	0	0	0
Quartz	0.4	0.4	0.4	0.6	0.2	0.2

X-ray diffraction (XRD) patterns were recorded over the range 3−65º2θ, using a Siemens D5000 diffractometer, equipped with a diffracted-beam monochromator. CuKα radiation was used for the measurements. Counting time was 5 s for the untreated and 10 s for the other samples per 0.025º2θ step.

The quantitative work was done with the AutoQuan software using a Lorentz function together with a polynomial of fifth order for background subtraction (Seifert Analytical X-ray, AutoQuan, version 2.7.0.0, 2006). Single-line fitting of the 001 and 060 Bragg peaks was carried out using the TOPAS V3.0 software from Bruker utilizing a Pseudo-Voigt profile function and a 3rd order polynomial as background.

A Genesys 10UV spectrophotometer from Thermoelectron Corp. was used to measure the RI values. The transmission was measured at a wavelength of 589.6 nm (Na D_1-line). The background was determined by measuring an empty, air-filled capillary of 1.5 mL volume.

For the RI mixture, two liquids were mixed: 2-Propanol (Merck Art. Nr. 109 634) with n = 1.385 and cinnamon aldehyde from Merck KGaA (Merck Art. Nr. 802 505) with n = 1.6219. Six mixtures in the volume ratio ranging from 0 to 100% in 20% steps were prepared.

Samples containing 30 mg were dispersed into the RI mixture with a total volume of 2 mL. The suspensions were ultrasonified for no more than 5 min to avoid a temperature increase in the suspension, and a concomitant change in the RI of the suspension. For more details see Weidler and Friedrich (2007).

The relationship between transmission intensity and RI was described by a Gauss function:

$$I = b + A \times \left(-\frac{(RI_s - RI_m)}{(2 \times \sigma)^2} \right) \quad (1)$$

with b = baseline, A = amplitude, RI_s = RI of the immersion oil, RI_m = RI of the mineral, and σ = parameter related to the width of the Gauss curve. This simple function is easy to apply and is often used in the fitting of transmission data (Bergmann and Schäfer, 1999). Nussbaumer *et al.* (2005) showed that the determination of the RI is very robust in terms of the mathematical method applied (*e.g.* Lorentz, Gauss, or polynomial function).

RESULTS AND DISCUSSION

Characterization and acid treatment

Because this sample is a natural product, it contained additional minerals. Rietveld analysis of the untreated sample revealed that kaolinite, phlogopite, calcite, albite, and traces of quartz were present (Table 1).

The illite was treated with 5 M HCl for periods between 2 and 24 h. During this treatment, the illite lost Fe, mainly situated in octahedral positions. This resulted

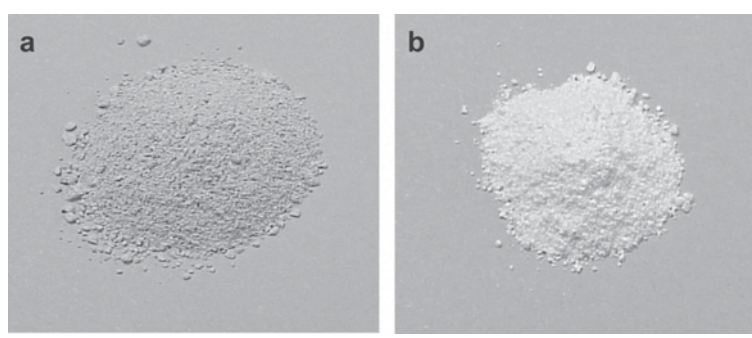

Figure 1. Photo of illite sample before (a) and after (b) a 24 h treatment with 5 M HCl.

Table 2. Changes in lattice parameter b_0 derived from the 060 peak and in the RI with Fe released from illite after acid treatment (h). The regression coefficients (R^2) obtained from fitting the RI data to the Gauss (equation 1) are added.

Duration (h)	b_0 (nm)	Fe Released (wt.% Fe_2O_3)	RI	R^2
0	0.9024	0	1.587	1.000
2	0.9005	2.0	1.562	0.994
4	0.8988	3.4	1.543	0.979
8	0.8983	4.4	1.527	0.991
12	0.8982	5.6	1.512	0.999
24	0.8978	6.2	1.502	0.997

Table 3. Change in d_{001} peak areas of illite and kaolinite during acid treatment, together with their ratios and the FWHM of the kaolinite d_{001} peak.

Duration (h)	Peak area of illite (a.u.)	Peak area of kaolinite (a.u.)	Peak area ratio for illite/ kaolinite	FWHM kaolinite
0	121.1	40.0	3.0	0.394
2	92.1	43.4	2.1	0.336
4	70.1	39.8	1.8	0.312
8	60.5	47.4	1.3	0.341
12	42.8	50.4	0.8	0.339
24	25.6	58.0	0.4	0.331

in a change in color of the clay powder from grayish/ greenish to white (Figure 1).

The illite lost 78% of its original Fe content within 24 h. Expressed in wt.% Fe_2O_3, the value decreased from 7.9 wt.% to 1.7 wt.% .

Fe in octahedral sites leads to an increased b_0 lattice parameter (Heller-Kallai and Rozenson, 1981). During partial dissolution, the b_0 lattice parameter decreased linearly from 0.9024 nm to 0.8978 nm with released Fe (Table 2), with a linear correlation coefficient (R) of −0.968** (probability level of 5%). Furthermore, the acid treatment had a strong effect on a number of minerals (Figure 2). Within the first 2−4 h of acid attack, all of the apatite, calcite, and phlogopite were removed (Table 1). According to the decrease in intensity of the d_{001} peak, the acid treatment also had an impact on illite, while, over the entire remaining duration of the dissolution, no significant changes in the

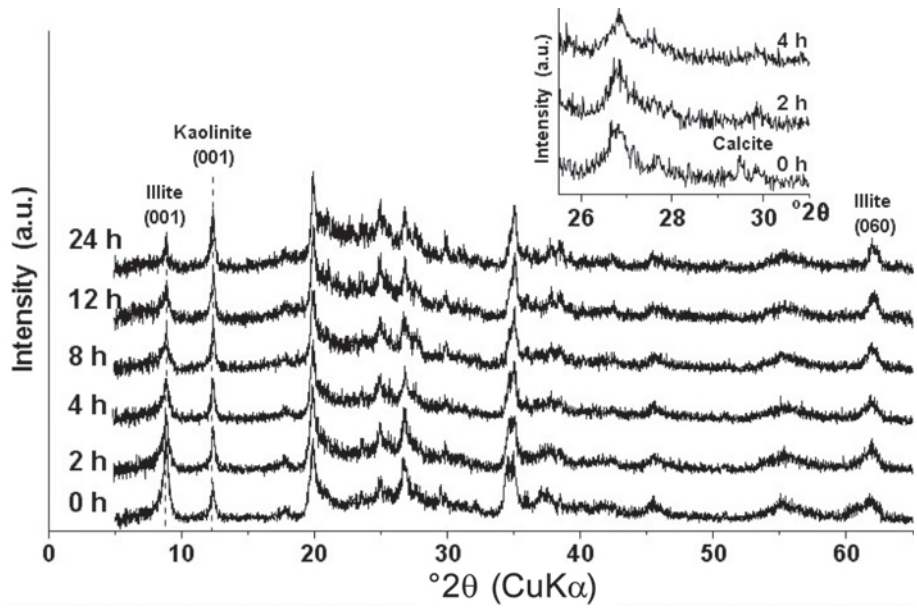

Figure 2. XRD patterns of the untreated and acid-treated illite.

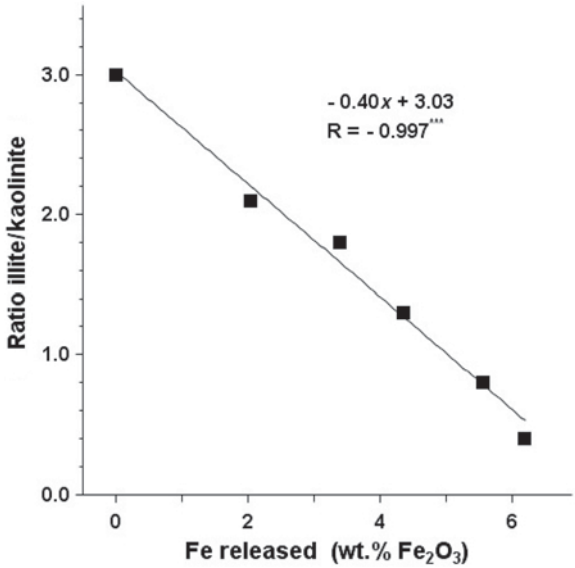

Figure 3. Change in the illite/kaolinite 001 peak-area ratio with decreasing Fe content in illite expressed as wt.% Fe_2O_3 released.

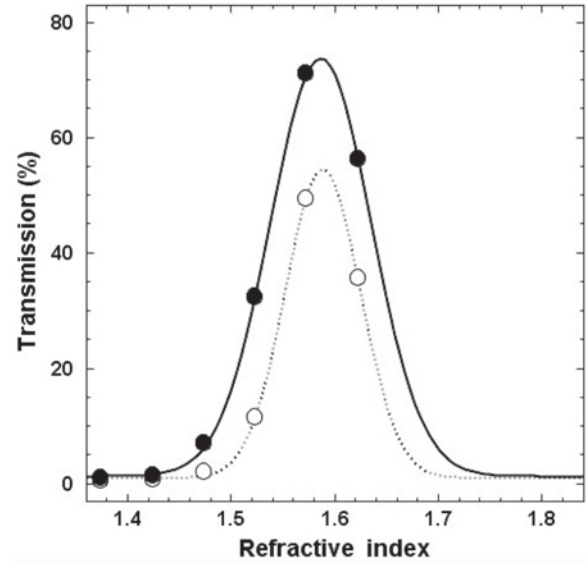

Figure 4. Transmission intensity plotted *vs.* the RI of the suspension liquid for the untreated illite sample. There were two independent preparations: ●: 1st run; ○: 2nd run.

kaolinite structure were detected. This was confirmed by the full width at half maximum values (FWHMs) of its d_{001} peak, which showed no significant variation during the acid treatment (Table 3). The degree of illite dissolution was determined by comparison of the d_{001} peak area with the d_{001} peak area of kaolinite (Table 3). This comparison suggested that 66 wt.% of the illite was dissolved after 24 h. This is in good agreement with the Fe loss from the illite, determined by the b_0 dimension. Moreover, the loss of Fe had no significant effect on the layered structure of the illite (existence of a sharp d_{001} peak even after 24 h of acid treatment).

The dependency of the d_{001} peak area ratios on Fe released is shown in Figure 3. The linear relationship demonstrates that most of the Fe released was situated in the illite structure.

Determination of the RI

The RI measurement took only a few minutes for six RI mixtures. The RI values of the untreated illite were 1.586 and 1.588 for two independent preparations (see Table 4 and Figure 4), and compared very well with literature data (Table 4). This RI value was closer to the β value. This finding could not be assigned unambiguously to an orientation of the particles in suspension. On one hand, this value was close to a mean value of 1.585 which is obtained for a completely random distribution of the principal vibrational directions (Wilcox, 1984). For the monoclinic crystal system these nearly coincide with the crystallographic axis, where n_α is almost parallel to the *c* axis and is perpendicular to the cleavage plane (Figure 5).

On the other hand, this could also be explained by the clay particles being oriented with their edges toward the transmitted light beam. Moreover, if the particles were oriented with their basal plane toward the light beam, the average RI value would have been somewhere between n_β and n_γ.

Because such preferred orientation of the particles was very unlikely due to the ultrasonic treatment prior to the measurement, the first interpretation was favored.

Hence, the mean RI values found using this method are appropriate for applications where these particles are suspended in a more or less random orientation, *e.g.* polymers as used in nanocomposites.

Table 4. Comparison of values of RI given by Jasmund and Lagaly (1993) and Tröger (1982) with those measured in the present study.

Mineral	n_α or n_ε	n_β or n_ω	n_γ	
Kaolinite	1.553–1.563	1.559–1.569	1.560–1.570	biaxial
Calcite	1.486–1.550	1.658–1.740		uniaxial
Quartz	1.552–1.554	1.543–1.545		uniaxial
Illite	1.568–1.572	1.587–1.590	1.590–1.600	biaxial
Illite 1st run		1.586		
Illite 2nd run		1.588		

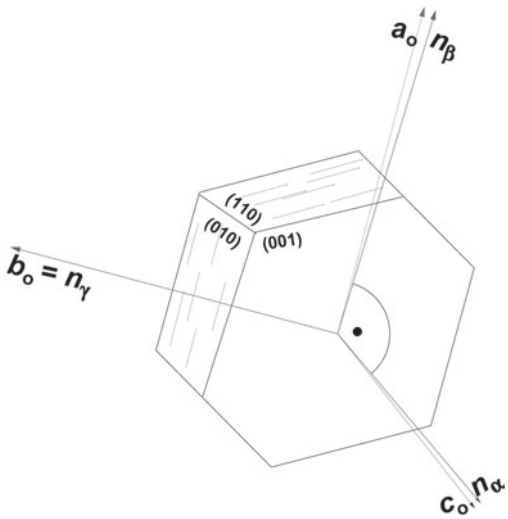

Figure 5. Correlation of crystal axis relative to the axis of the refractive indices (sketch according to Wilcox, 1984).

The Gaussian fits to the transmission data of the RI suspensions containing the acid-treated samples (Figure 6, Table 2) were all excellent. The RI of the illite decreased with duration of the acidic treatment.

The relationship between this RI value and the Fe content of the illite is clear (Figure 7). The linear relationship was in accord with that established by theoretical means, *i.e.* the decrease in RI depended on dissolution of Fe from octahedral positions of the illite.

Adjustment of the RI in a very precise manner is, therefore, possible for conditions required by the matrix. This also implies that the strict grain-size requirements for applications in transparent systems are avoided by means of adjustment of the RI.

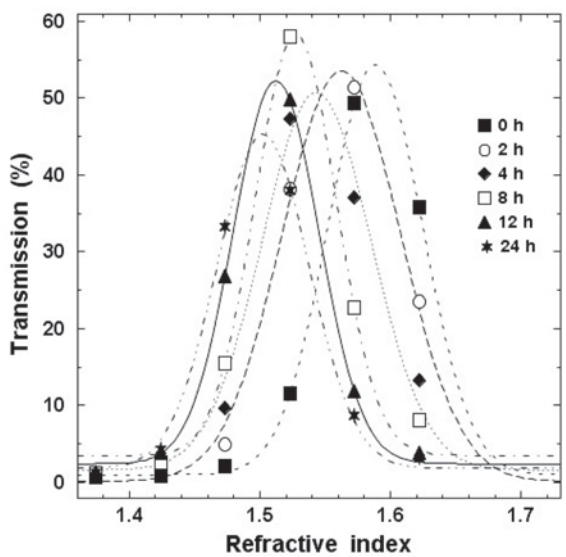

Figure 6. Transmission intensity plotted *vs.* the RI of the suspension liquid for the starting material and acid-treated samples.

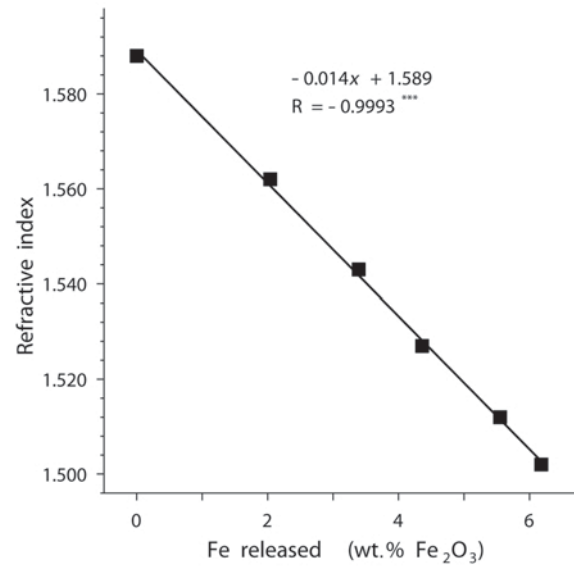

Figure 7. Change in the RI with decreasing Fe content in illite expressed as wt.% Fe_2O_3 released.

CONCLUSION

This study showed that the RI of illite can be adjusted to a certain degree without destroying its layer structure. The change in RI is, at first approximation, a linear function of the Fe removed from octahedral sites by acid attack.

ACKNOWLEDGMENTS

PGW thanks the Danish Research Council for Technology and Production for supporting the research visit at IGV by means of grant no. 274-06-0053.

REFERENCES

Alexandre, M. and Dubois, P. (2000) Polymer-layered silicate nanocomposites: Preparation, properties and uses of a new class of materials. *Materials Science and Engineering*, **28**, 1–63.

Aranda, P., Darder, M., Fernández-Saavedra, R., Lopez-Blanco, M., and Ruiz-Hitzky, R. (2006) Relevance of polymer- and biopolymer-clay nanocomposites in electrochemical and electroanalytical applications. *Thin Solid Films*, **495**, 104–112.

Avella, M., De Vlieger, J.J., Errico, M.E., Fischer, S., and Volpe, M.G. (2005) Biodegradable starch/clay nanocomposite films for food packaging applications. *Food Chemistry*, **93**, 467–474.

Bergmann, L. and Schaefer, C. (1999) *Optics of Waves and Particles*. Walter de Gruyter, New York, 1400 pp.

Bloss, F.D. (1999) *Optical Crystallography*. Mineralogical Society of America, Washington, D.C., 239 pp.

Feynman, R.P., Leighton, R.B., and Sand, M. (1991) *Feynman Vorlesungen über Physik, Bd. II: Hauptsächlich Elektromagnetismus und Struktur der Materie*. R. Oldenbourg Verlag, München, Vienna, 851 pp.

Gilg, H.A., Haus, R., and Frei, R. (1997) A new illite deposit near le-Puy-en-Velay (France) – genesis and usage for waste encapsulation. Pp. 717–720 in: *Mineral Deposits: Research and Exploration – Where do they Meet?* (H.

Papunen, editor). Procedings of the 4th Biennial SGA Meeting, Turku, Finland, Balkema Press, Rotterdam.

Heller-Kallai, L. and Rozenson, I. (1981) The use of Mössbauer spectroscopy of iron in clay mineralogy. *Physics and Chemistry of Minerals*, **7**, 223–238.

Jasmund, K. and Lagaly, G. (1993) *Tonminerale und Tone. Struktur, Eigenschaften, Anwendung und Einsatz in Industrie und Umwelt*. Steinkopff Verlag, Darmstadt, Germany, 490 pp.

Köhler, S.J., Dufaud, D., and Oelkers, E.H. (2003) An experimental study of illite dissolution kinetics as a function of pH from 1.4 to 12.4 and temperature from 5 to 50ºC. *Geochimica et Cosmochimica Acta*, **6**, 3583–3594.

Nussbaumer, R.J., Halter, M., Tervoort, T., Caseri, W.R., and Smith, P. (2005) A simple method for the determination of refractive indices of (rough) transparent solids. *Journal of Materials Science*, **40**, 575–582.

Okada, A. and Usuki, A. (2006) Twenty years of polymer-clay nanocomposites. *Macromolecular Materials and Engineering*, **291**, 1449–1476.

Rhim, J.W. and Ng, P.K.W. (2007) Natural biopolymer-based nanocomposite films for packaging applications. *Critical Reviews in Food Science and Nutrition*, **47**, 411–433.

Scott, A.D. and Smith, S.J. (1966) Susceptibility of interlayer potassium in micas to exchange with sodium. C*lays and Clay Minerals*, **14**, 69–81.

Tetsuka H., Ebina T., Nanjo H., and Mizukami, F. (2007) Highly transparent flexible clay films modified with organic polymer: Structural characterization and intercalation properties. *Journal of Materials Chemistry*, **17**, 3545–3550.

Tröger, W.E. (1982) *Optische Bestimmung der gesteinsbildende Minerale. Teil 1: Bestimmungstabellen*. 3rd edition, Schweizerbartsche Verlagsbuchhandlung, Stuttgart, Germany, 188 pp.

Weidler, P.G. and Friedrich, F. (2007) Determination of the refractive index of particles in the clay and sub-µm size range. *American Mineralogist*, **92**, 1130–1132.

Wilcox, R.E. (1983) Refractive index determination using the central focal masking technique with dispersion colors. *American Mineralogist*, **68**, 1226–1236.

Wilcox, R.E. (1984) Optical properties of mica under the polarizing microscope. Pp. 183–200 in: *Micas* (S.W. Bailey, editor). Reviews in Mineralogy, **13**. Mineralogical Society of America, Washington, D.C.

Zeng, Q.H., Yu, A.B., Lu, G.Q., and Paul, D.R. (2005) Clay-based polymer nanocomposites: research and commercial development. *Journal of Nanoscience and Nanotechnology*, **5**, 1574–1592.

(*Received 24 May 2007; revised 20 June 2008; Ms. Ms 0036; A.E. R.E. Ferrell*)